Bralower, T.J., Premoli Silva, I., and Malone, M.J. (Eds.)
Proceedings of the Ocean Drilling Program, Scientific Results Volume 198

14. Data Report: Opal and Carbonate Data from the Miocene to Lower Pliocene, Site 1208 (Central High, Shatsky Rise)[1]

Stuart A. Robinson[2,3] and Hugh C. Jenkyns[4]

ABSTRACT

Weight percent opal and carbonate data are presented for the Miocene–Lower Pliocene interval at Site 1208 on Shatsky Rise. These data compare favorably with shipboard estimates and measurements. The opal and carbonate data confirm that the color cycles recognized in shipboard data are the result of fluctuations in carbonate content and are not related to opal productivity.

INTRODUCTION

Hole 1208A is the only drill hole on the Central High of Shatsky Rise. Unlike the Southern High of Shatsky Rise, the Central High has an expanded Neogene (lower Miocene–Holocene) section, ~300 m thick at Ocean Drilling Program Site 1208. Cyclicity is evident throughout the Neogene sediments in total reflectance (L*) and magnetic susceptibility data. The Miocene cycles are especially striking with clear decimeter- to meter-scale alternations in color. The light-colored intervals consist of nannofossil ooze/chalk, whereas the dark intervals comprise nannofossil clays and claystones. The contacts between the color cycles are either gradational or bioturbated. Shipboard analysis of the color cycles in the Miocene–Pliocene suggests that the dominant period of the cycles corresponds to obliquity (41 k.y.) prior to 0.8 Ma (Bralower, Premoli Silva, Malone, et al., 2002) with the cycles interpreted as the

[1] Robinson, S.A., and Jenkyns, H.C., 2005. Data report: Opal and carbonate data from the Miocene to Lower Pliocene, Site 1208 (Central High, Shatsky Rise). *In* Bralower, T.J., Premoli Silva, I., and Malone, M.J. (Eds.), *Proc. ODP, Sci. Results,* 198, 1–7 [Online]. Available from World Wide Web: <http://www-odp.tamu.edu/publications/198_SR/VOLUME/CHAPTERS/120.PDF>. [Cited YYYY-MM-DD]
[2] School of Human and Environmental Sciences, University of Reading, Whiteknights, PO Box 227, Reading RG6 6AB, United Kingdom.
s.a.robinson@reading.ac.uk
[3] Lamont-Doherty Earth Observatory of Columbia University, 61 Route 9W, Palisades NY 10964, USA.
[4] Department of Earth Sciences, University of Oxford, Parks Road, Oxford OX1 3PR, United Kingdom.

Initial receipt: 30 November 2004
Acceptance: 16 May 2005
Web publication: 2 September 2005
Ms 198SR-120

consequence of variations in productivity and/or carbonate dissolution. Furthermore, Bralower, Premoli Silva, Malone, et al. (2002) postulated that higher surface water productivity and higher clay input from zonal winds could explain the origin of the dark cycles. We present initial results that document the sedimentary composition (weight percent opal and carbonate) of the cyclic lithologies.

METHODS AND MATERIALS

The 78 samples used in this study were originally collected on board the *JOIDES Resolution* from Cores 198-1208A-22X through 35X (~190–320 meters below seafloor [mbsf]) spanning the Lower Pliocene–lower Miocene. The 78 samples were originally used for the shipboard measurement of moisture and density properties, during which the samples were oven-dried at ~100°C for 24 hr (see Bralower, Premoli Silva, Malone, et al., 2002).

Carbonate

Carbonate analyses were performed using a Coulometric, Inc., carbon dioxide coulometer. In this technique, ~5 mg of sample is reacted with 4.0 mL of 2-M HCl to release CO_2 that then passes through a solution containing monoethanolamine and a colorimetric indicator. CO_2 and monoethanolamine react to form a titratable acid (hydroxyethylcarbamic acid), which causes the color indicator to fade. Photodetection monitors the change in the color of the solution. As the color changes, the titration current is automatically activated to stoichiometrically generate base (alkali) at a rate proportional to the color change, thereby returning the solution to the original color, at which point the current stops. Weight percent inorganic carbon is proportional to the titration current. Reproducibility of an internal standard was approximately ±1%.

Opal

The method used here follows that of Mortlock and Froelich (1989). On the basis of color and carbonate content, between 50 and 150 mg of powdered sample was used. Carbonate and organics were removed using 10% HCl and 10% H_2O_2, respectively. Biogenic silica was then extracted using a solution of 2-M Na_2CO_3 for 5–8 hr. The resulting solution was diluted with molybdate solution and the absorbency of each sample was measured using a spectrophotometer. The absorbance is proportional to the silica concentration, thereby allowing calculation of weight percent silica and opal. Reproducibility of the absorbance measurements (and hence silica concentrations) was typically better than ±6%, and in almost all cases was better than ±4%.

RESULTS

Results are listed in Table T1 and shown in Figures F1 and F2. Figure F1 shows the downhole trends in L* (for the samples analyzed), carbonate, and opal. Our new carbonate data range in value from 18.5 to 90.8 wt%, which is in good agreement with the values measured on the ship for this same depth interval (range = 9.8–89.3 wt%). The opal content

T1. Opal and carbonate data, p. 7.

F1. L*, opal, and carbonate data, p. 5.

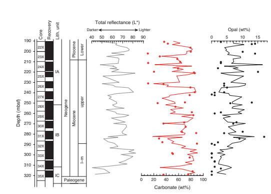

F2. L*, opal, and carbonate cross-plots, p. 6.

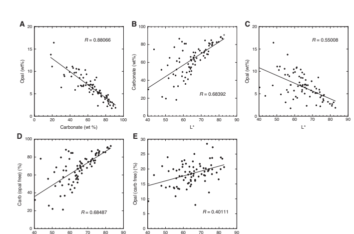

of the bulk sediments generally agrees well with the estimates from smear slides. In the interval from 190 to 290 mbsf, measured opal values are highly variable (2.3–16.4 wt%). Below 290 mbsf, opal values are generally low (1.8–7 wt%). It is clear from Figure F1 that darker sediments are generally characterized by decreased carbonate contents and increased opal contents. A crossplot shows a negative linear relationship between carbonate and opal (Fig. F2A). A crossplot of carbonate against total reflectance (Fig. F2B) confirms the shipboard observation that carbonate contents are highest in the lighter-colored sediments. A weak linear correlation is found between opal and total reflectance (Fig. F2C), suggesting that although opal is generally more abundant in the darker sediments, it is not necessarily intimately related to the color cycles. In order to understand the role of carbonate dilution of any opal signal, it is particularly instructive to consider opal corrected for carbonate content and carbonate corrected for opal content (i.e., for opal, by calculating the relative proportions of opal and terrigenous sediment without carbonate, adding up to 100%). Figure F2D shows that removal of the opal component has little or no effect on the relationship between carbonate and total reflectance. However, Figure F2E clearly shows that removal of the carbonate component results in very different relationship between opal and total reflectance (cf. Fig. F2C). These results suggest that the color cycles are primarily the result of fluctuations in carbonate content and that the fluctuations in opal content are primarily the result of dilution by carbonate and not a primary signal.

SUMMARY

Carbonate and opal data from the Neogene at Site 1208 display downhole trends that are correlated with downhole trends in L*. The trends in L* are most likely controlled by the abundance of carbonate.

ACKNOWLEDGMENTS

This research used samples and/or data provided by the Ocean Drilling Program (ODP). ODP is sponsored by the U.S. National Science Foundation (NSF) and participating countries under management of Joint Oceanographic Institutions (JOI), Inc. S.A. Robinson acknowledges the support of United Kingdom ODP (UKODP) for funding his participation aboard Leg 198. This work was funded by grants to the authors from the National Environment Research Council (NER/T/S/2001/01240) and UKODP (Rapid Response Grant). We acknowledge the assistance in the laboratory of Pat Malone and Linda Baker at the Lamont-Doherty Earth Observatory.

REFERENCES

Bralower, T.J., Premoli Silva, I., Malone, M.J., et al., 2002. *Proc. ODP, Init. Repts.,* 198 [CD-ROM]. Available from: Ocean Drilling Program, Texas A&M University, College Station TX 77845-9547, USA.

Mortlock, R.A., and Froelich, P.N., 1989. A simple method for the rapid determination of biogenic opal in pelagic marine sediments. *Deep-Sea Res., Part A,* 36:1415–1426.

Figure F1. Lithostratigraphic, core recovery, color reflectance (from Bralower, Premoli Silva, Malone, et al., 2002), opal, and carbonate data. Solid circles are shipboard measurements of opal (smear slides) and carbonate (coulometry) from Bralower, Premoli Silva, Malone, et al. (2002).

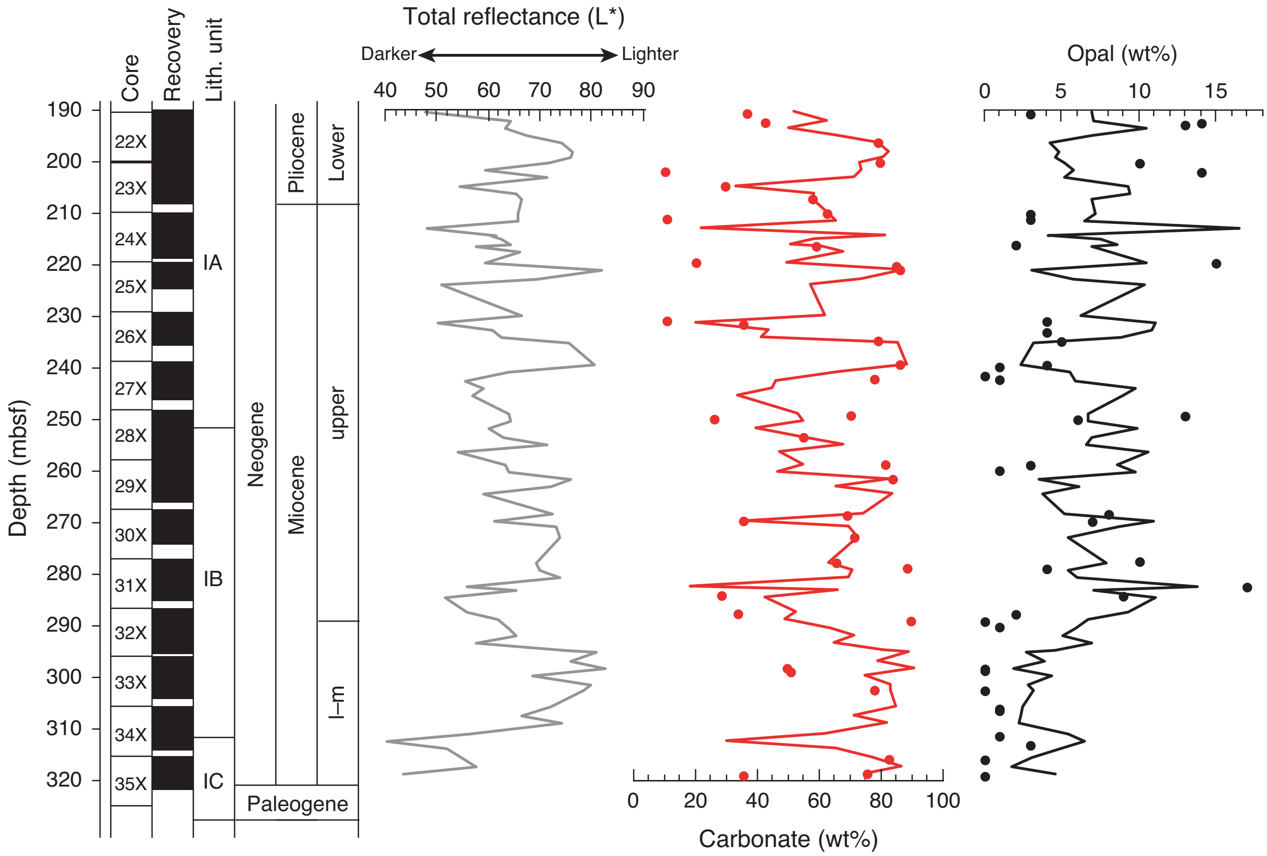

Figure F2. Crossplots of (**A**) opal vs. carbonate, (**B**) carbonate vs. L* (total color reflectance), (**C**) opal vs. L*, (**D**) carbonate (opal free) vs. L*, and (**E**) opal (carbonate free) vs. L*.

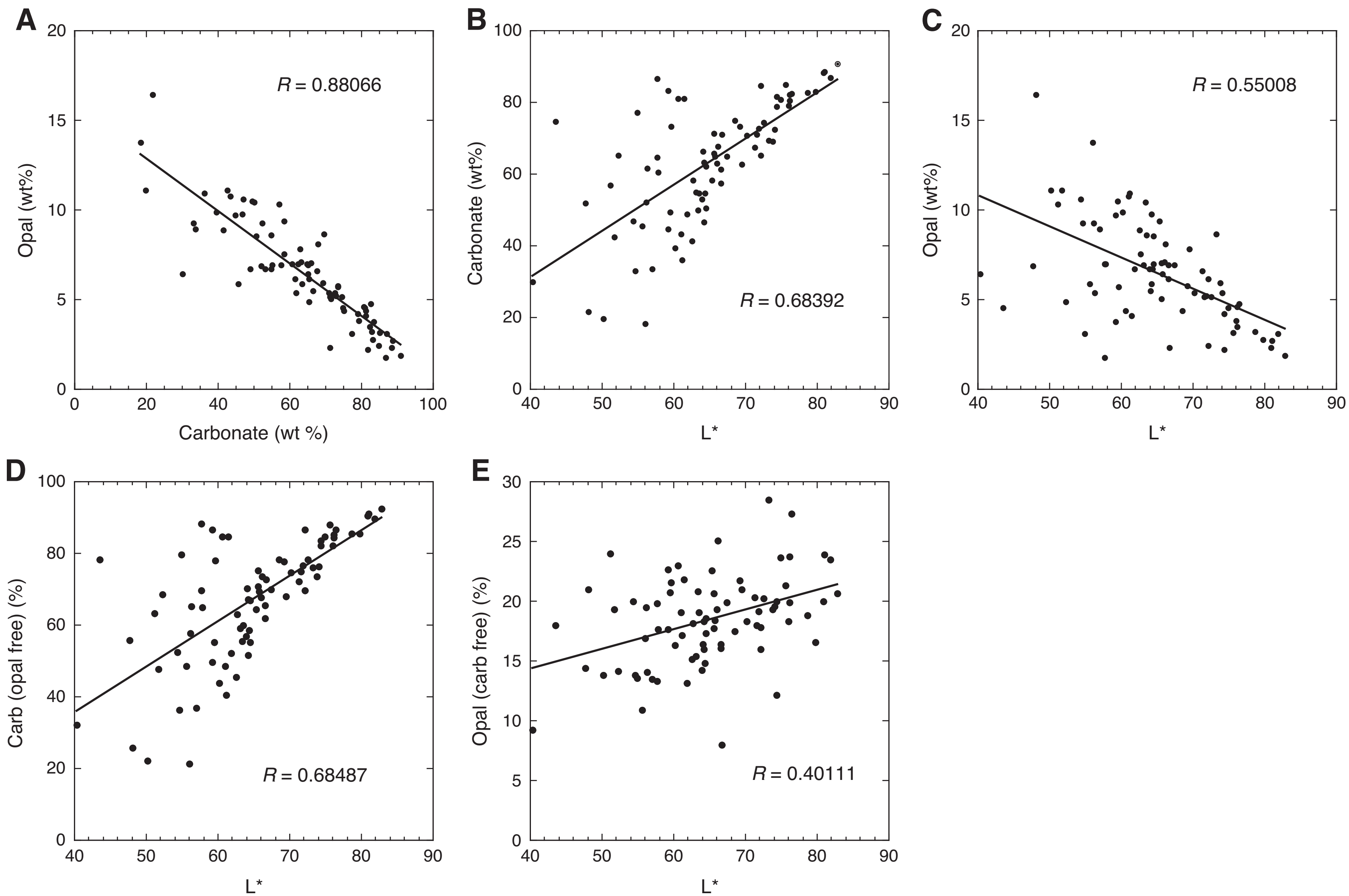

Table T1. Opal and carbonate data.

Core, section, interval (cm)	Depth (mbsf)	Opal (wt%)	Carbonate (wt%)
198-1208A-			
22X-1, 13–15	190.53	6.89	52.07
22X-2, 13–15	192.03	7.03	62.17
22X-3, 13–15	193.53	10.42	49.89
22X-4, 13–15	195.03	6.96	65.04
22X-5, 13–15	196.53	4.25	78.77
22X-6, 13–15	198.03	4.78	82.54
22X-7, 13–15	199.23	4.59	80.69
23X-1, 11–13	200.21	5.22	72.75
23X-2, 11–13	201.71	5.72	73.47
23X-3, 11–13	203.21	5.19	71.12
23X-4, 11–13	204.71	9.27	32.98
23X-5, 11–13	206.21	9.40	58.31
23X-6, 11–13	207.21	6.95	57.61
24X-1, 18–20	209.98	7.13	63.09
24X-2, 13–15	211.43	6.43	65.07
24X-3, 13–15	212.93	16.44	21.65
24X-3, 146–148	214.25	4.11	81.15
24X-4, 13–15	214.43	4.37	81.03
24X-4, 88–90	215.18	7.56	58.38
24X-5, 12–14	215.93	8.56	50.65
24X-5, 53–55	216.32	7.00	60.45
24X-6, 18–20	217.48	8.09	67.78
25X-1, 21–23	219.60	10.50	49.43
25X-2, 8–10	220.98	3.10	86.82
25X-3, 33–35	222.73	5.79	73.35
25X-4, 14–16	223.73	10.35	56.83
26X-1, 65–67	229.75	6.19	61.54
26X-2, 68–70	231.28	11.12	19.76
26X-3, 51–53	232.61	10.79	43.46
26X-4, 45–47	234.05	8.88	41.42
26X-5, 40–42	234.95	3.16	85.15
27X-1, 78–80	239.48	2.32	88.37
27X-2, 68–70	240.88	5.52	66.36
27X-3, 69–71	242.39	5.91	45.68
27X-4, 70–72	243.90	9.74	44.83
27X-5, 70–72	245.40	8.95	33.71
28X-1, 68–70	248.77	6.70	53.09
28X-2, 68–70	250.27	6.72	54.64
28X-3, 66–68	251.75	9.87	39.47
28X-4, 68–70	253.27	6.95	55.00
28X-5, 69–71	254.80	6.60	67.58
28X-6, 71–73	256.30	10.63	46.86
29X-1, 78–80	258.58	8.63	54.82
29X-2, 75–77	260.05	9.77	46.72
29X-3, 73–75	261.53	3.52	82.34
29X-4, 68–70	262.98	6.17	65.41
29X-5, 64–66	264.44	3.76	83.41
30X-1, 68–70	268.08	5.19	74.36
30X-2, 78–80	269.68	10.93	36.24
30X-3, 32–34	270.72	8.69	69.53
30X-4, 92–94	272.82	5.40	72.40
31X-1, 70–72	277.70	7.83	62.71
31X-2, 53–55	279.03	5.37	70.74
31X-3, 70–72	280.70	5.95	69.16
31X-4, 73–75	282.23	13.80	18.45
31X-5, 20–22	283.2	7.07	65.84
31X-6, 28–30	284.28	11.11	42.59
32X-1, 70–72	287.30	9.28	52.36
32X-2, 70–72	288.80	6.74	48.83
32X-3, 69–71	290.29	5.87	63.30
32X-4, 73–75	291.83	5.08	71.42
32X-5, 67–69	293.27	6.99	64.82
32X-6, 52–54	294.62	4.54	80.81
32X-6, 85–87	294.95	2.71	88.66
33X-1, 70–72	296.60	3.83	79.06
33X-2, 70–72	298.10	1.90	90.82
33X-3, 70–72	299.60	4.39	74.93
33X-4, 77–79	301.17	2.79	83.17
33X-5, 66–68	302.56	3.22	82.88
34X-1, 13–15	305.73	2.45	84.68
34X-2, 27–29	307.37	2.31	71.17
34X-3, 17–19	308.77	2.23	81.67
34X-4, 77–79	310.87	5.41	61.64
34X-5, 57–59	312.17	6.47	30.13
34X-6, 64–66	313.74	4.92	65.38
35X-1, 31–33	315.61	3.11	77.16
35X-2, 33–35	317.13	1.78	86.65
35X-3, 47–49	318.77	4.55	74.68